Phonon-assisted relaxation kinetics of statistically degenerate excitons in high-quality quantum wells

A. V. Soroko* and A. L. Ivanov
Department of Physics and Astronomy, Cardiff University, Cardiff CF24 3YB, Wales, United Kingdom
(Received 25 October 2001; published 4 April 2002)

Acoustic-phonon-assisted thermalization kinetics of excitons in quantum wells (QW's) is developed for small concentrations of particles, $\rho_{2D} \lesssim 10^9$ cm^{-1}, when particle-particle interaction can be neglected, while Bose-Einstein statistics already strongly influences the relaxation processes at low temperatures. In this case thermalization of QW excitons occurs through nonequilibrium states and is given by the following scenario. During the first transient stage, which lasts a few characteristic scattering times, the correlations with an initial distribution of QW excitons disappear. The next, adiabatic stage of thermalization usually takes many characteristic scattering times, depends only upon two control parameters, the lattice temperature T_b and the degeneracy temperature $T_0 \propto \rho_{2D}$, and is characterized by a quasiequilibrated distribution of high-energy QW excitons with effective temperature $T(t)$. We show that the thermalization law of high-energy particles is given by $\delta T(t) = T(t) - T_b \propto e^{-\lambda_0 t}/t$, where λ_0 is a marginal value of the continuous eigenvalue spectrum of the linearized kinetics. By analyzing the linearized phonon-assisted kinetics of statistically degenerate QW excitons, we study the dependence $\lambda_0 = \lambda_0(T_b, T_0)$. Our numerical estimates refer to high-quality GaAs and ZnSe QW's. Finally, we propose a special design of GaAs-based microcavities, which considerably weakens the bottleneck effect in relaxation of excitons (polaritons) and allows us to optimize the acoustic-phonon-assisted thermalization processes.

DOI: 10.1103/PhysRevB.65.165310 PACS number(s): 78.66.−w, 72.10.Di, 63.20.Kr

I. INTRODUCTION

The formation, resonant or phonon assisted, of quantum-well (QW) excitons and their following relaxation towards a final (quasi-) equilibrium thermodynamic state at low lattice temperature T_b are the subject of numerous experimental[1] and theoretical[2–9] studies. Recently, relaxation thermodynamics has been formulated and developed in order to analyze how Bose-Einstein statistics of high-density QW excitons influences the phonon-assisted thermalization processes.[10] The above thermodynamics assumes a strong, dominant exciton-exciton scattering and, therefore, relaxation through quasiequilibrium thermodynamic states. The relaxation thermodynamics has successfully been applied to model the ρ_{2D}-dependent thermalization and photoluminescence kinetics observed in early experiments[11,12] with high-density excitons (5×10^9 cm$^{-2} \lesssim \rho_{2D} \lesssim 10^{11}$ cm^{-2}) in GaAs QW's.[10]

The long-lived indirect excitons in high-quality GaAs/Al$_x$Ga$_{1-x}$As-coupled QW's provide a unique opportunity for studying quantum degeneracy in a system of two-dimensional bosons. In this case, the long radiative lifetimes of indirect excitons allow the system to cool down to temperatures where the dilute exciton gas becomes statistically degenerate.[13–20] The quality of present-day GaAs/Al$_x$Ga$_{1-x}$As-coupled QW's has been considerably improved in comparison with those used in the pioneering experiments[13,21–25] decade ago.[26] Furthermore, the very recent magneto-optical experiments[27] clearly indicate that the in-plane momentum $\hbar \mathbf{k}_\parallel$ of indirect excitons is a well-defined quantum number in high-quality GaAs/Al$_x$Ga$_{1-x}$As-coupled QW's.

Thermalization of hot photoexcited excitons down to the temperature of the cold lattice occurs mainly via scattering by thermal bulk longitudinal acoustic (LA) phonons and is much more efficient for quasi-two-dimensional (quasi-2D) systems as compared to bulk semiconductors. This follows from the relaxation of momentum conservation in the z direction (the QW growth direction) for quasi-2D systems: the ground-state mode $\mathbf{k}_\parallel = \mathbf{0}$, i.e., the energy state $E = 0$, couples to the continuum energy states $E \geqslant E_0$, rather than to the single energy state $E = E_0 = 2M_x v_s^2$ (v_s is the longitudinal sound velocity and M_x is the in-plane translational mass of excitons) as occurs in bulk materials. As a result, the LA-phonon-assisted kinetics of QW excitons becomes dominant at $\rho_{2D} \lesssim (1-3) \times 10^9$ cm^{-2}: in this case exciton-exciton scattering can be neglected while Bose-Einstein (BE) statistics already strongly influences the relaxation process at low temperatures.[10] Crossover from classical to quantum statistics occurs near the degeneracy temperature $k_B T_0 = (2\pi\hbar^2 \rho_{2D})/(g M_x)$, where g is the spin-degeneracy factor. For $\rho_{2D} = 3 \times 10^9$ cm^{-2} the degeneracy temperature of indirect excitons in GaAs/Al$_x$Ga$_{1-x}$As-coupled QW's is $T_0 = 0.79$ K. This estimate refers to $g = 1$, which can be achieved in the b-type GaAs/Al$_x$Ga$_{1-x}$As-coupled QW's by applying a static magnetic field $\mathbf{H} \| \mathbf{z}$.[15] Note that the very recent experiments[18] deal with GaAs/Al$_x$Ga$_{1-x}$As-coupled QW's at extremely low cryostat temperature $T_b = 0.05$ K. Because the binding energy of indirect excitons in GaAs/Al$_x$Ga$_{1-x}$As-coupled QW's is about 3–5 meV,[27] for concentrations $\rho_{2D} \lesssim 10^9$ cm^{-2}, the Mott parameter is much less than unity, $\rho_{2D} a_x^2 \sim 0.001$ (a_x is the in-plane radius of an indirect exciton). In this case the ensemble of indirect excitons can be interpreted in terms of a rather dilute, nearly ideal quasi-2D gas of Bose particles.

In this paper we study analytically and model numerically

the acoustic-phonon-assisted relaxation kinetics of statistically degenerate QW excitons at low densities. The recent experiments[28,29] allow us to visualize, by means of LO-phonon-assisted emission, the LA-phonon-assisted kinetics of quasi-2D excitons in ZnSe QW's and, in particular, to prove that for $\rho_{2D} \lesssim 10^9$ cm^{-2} the above kinetics indeed occurs through nonequilibrium distributions of QW excitons. In experiments[14–16,18] the concentration of BE-degenerate indirect excitons in GaAs/Al$_x$Ga$_{1-x}$As-coupled QW's usually varies from $\rho_{2D} \gtrsim 10^{10}$ cm^{-2} at the very end of an optical excitation pulse to $\rho_{2D} \lesssim 10^8$ cm^{-2} at large delay times $t \gtrsim 50$ ns after the optical excitation. Thus, thermalization of the indirect excitons at large delay times cannot be described within the relaxation thermodynamics[10] and does need a separate theoretical analysis.

The classical Boltzmann kinetic equation has been generalized in order to include quantum statistics by Uehling and Uhlenbeck.[30] The relevant quantum kinetic equation for a spatially homogeneous dilute system of statistically degenerate quasi-2D excitons coupled to bulk LA phonons is

$$\frac{\partial}{\partial t} N_{\mathbf{k}_\parallel} = -\frac{2\pi}{\hbar} \sum_{\mathbf{q}} |M(q,q_z)|^2 \{ [N_{\mathbf{k}_\parallel}(1+n^{\rm ph}_{\mathbf{q}})(1+N_{\mathbf{k}_\parallel-\mathbf{q}_\parallel}) - (1+N_{\mathbf{k}_\parallel}) n^{\rm ph}_{\mathbf{q}} N_{\mathbf{k}_\parallel-\mathbf{q}_\parallel}] \delta(E_{\mathbf{k}_\parallel} - E_{\mathbf{k}_\parallel-\mathbf{q}_\parallel} - \hbar q v_s) + [N_{\mathbf{k}_\parallel} n^{\rm ph}_{\mathbf{q}} (1+N_{\mathbf{k}_\parallel+\mathbf{q}_\parallel}) - (1+N_{\mathbf{k}_\parallel}) \times (1+n^{\rm ph}_{\mathbf{q}}) N_{\mathbf{k}_\parallel+\mathbf{q}_\parallel}] \delta(E_{\mathbf{k}_\parallel} - E_{\mathbf{k}_\parallel+\mathbf{q}_\parallel} + \hbar q v_s) \}, \quad (1.1)$$

where $N_{\mathbf{k}_\parallel}$ and $n^{\rm ph}_{\mathbf{q}}$ are the occupation numbers of exciton in-plane mode $\mathbf{k}_\parallel$ and phonon bulk mode $\mathbf{q}=\{\mathbf{q}_\parallel, q_z\}$, respectively, and $\mathbf{q}_\parallel$ is the in-plane projection of $\mathbf{q}$. The terms in the first and second square brackets on the right-hand side (rhs) of Eq. (1.1) describe the Stokes and anti-Stokes LA-phonon-assisted scattering processes, respectively. The acoustical phonons are assumed to be in thermal equilibrium at the bath temperature T_b.[10] The matrix element is given by $M(q,q_z) = [(D_x^2 \hbar q)/(2\rho v_s V)]^{1/2} F_z(q_z L_z/2)$, where ρ is the crystal mass density, D_x is the deformation potential of the exciton–LA-phonon interaction, L_z is the thickness of a QW, and V is the volume. The form factor $F_z(\chi) = [\sin(\chi)/\chi][e^{i\chi}/(1-\chi^2/\pi^2)]$ refers to an infinite rectangular confinement potential.[31] The latter function describes the relaxation of the momentum conservation law in the z direction and characterizes a spectral band of bulk LA phonons, which effectively interact with QW excitons. Note that Eq. (1.1) is valid only for the kinetic stage of thermalization, i.e., before a low-temperature collective state of excitons[32–35] builds up.

The main aim of our work is to study the fundamental features of the acoustic phonon-assisted thermalization kinetics of QW excitons from initial strongly nonequilibrium $N_{\mathbf{k}_\parallel}(t=0)$ towards the final equilibrium distribution with well-developed Bose-Einstein statistics, when $N^0_{\mathbf{k}_\parallel=0} \gtrsim 1$. Our numerical simulations of the LA-phonon-assisted kinetics clearly demonstrate that after the first transient, which lasts a few characteristic scattering times, a slow *adiabatic stage* of thermalization builds up (see Fig. 1). This stage is characterized by a quasiequilibrium distribution of high-energy QW excitons with effective temperature $T(t) = T_b + \delta T(t)$ and is independent of the initial distribution at $t=0$. The adiabatic stage lasts many characteristic scattering times and arises due to the need to populate the low-energy in-plane modes with $N_{\mathbf{k}_\parallel \simeq \mathbf{0}} \gtrsim 1$ in the presence of effective suppression of the stimulated scattering processes (e.g., an intense incoming Stokes flux of excitons into the ground-

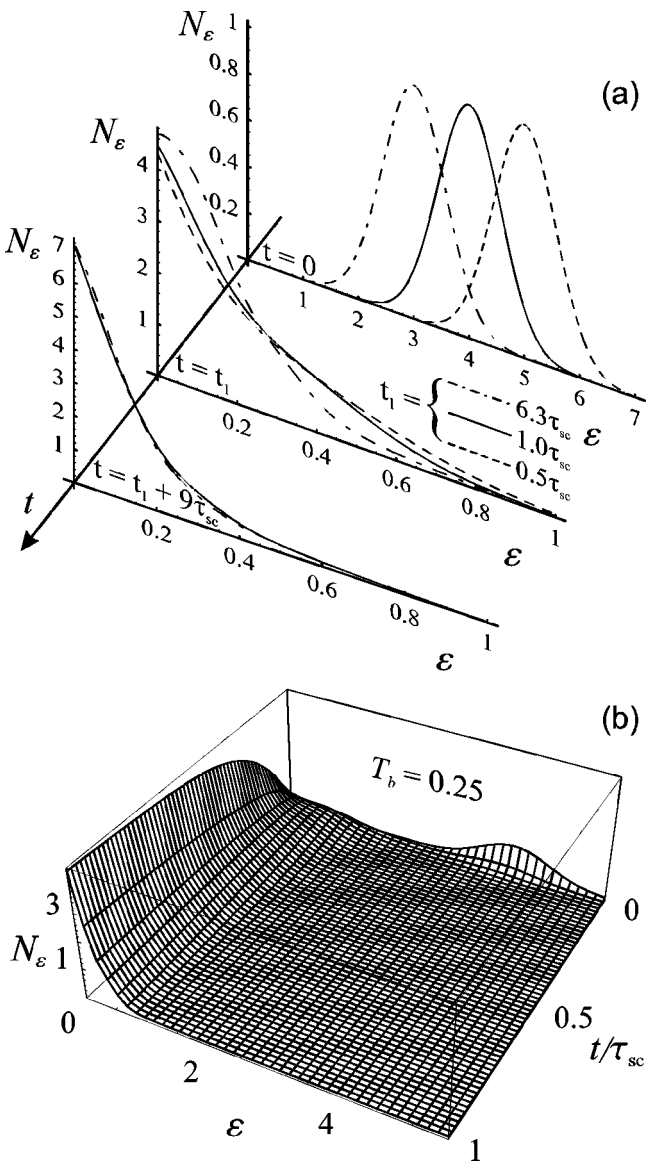

FIG. 1. (a) Transient relaxation towards the adiabatic stage of evolution calculated for various initial Gaussian distributions $N_\varepsilon(t=0) \propto \exp[-15.625(\varepsilon - \bar{\varepsilon})]$, where $\varepsilon = \hbar^2 \mathbf{k}_\parallel^2/(2M_x E_0)$, and parameter $\bar{\varepsilon} = 3$ (dash-dotted lines), 4 (solid lines), and 5 (dashed lines). The gross dependence of evolution upon initial conditions is absorbed by time $t_1 \simeq t_c$. (b) The first stage of LA-phonon-assisted relaxation ($t \lesssim \tau_{\rm sc}$) for a particular distribution of indirect excitons with $\bar{\varepsilon} = 4$. In both plots $T_b = 0.25$ and $T_0 = 1.14$. The dimensionless values, time in $\tau_{\rm sc}$ and energy/temperature in E_0, can easily be rescaled to dimensional units by using $E_0 = 33$ μeV and $\tau_{\rm sc} = 41$ ns for GaAs/Al$_x$Ga$_{1-x}$As-coupled QW's, and $E_0 = 162$ μeV and $\tau_{\rm sc} = 2.7$ ns relevant to ZnSe QW's.

state mode $\mathbf{k}_\parallel=0$ is nearly compensated by the outgoing anti-Stokes scattering out of the state $\mathbf{k}_\parallel=0$). In order to describe the adiabatic stage of relaxation, we find a *generic solution* of the quantum kinetic Equation (1.1). While the generic solution we calculate is different from that derived in Ref. 45 for the phonon-assisted kinetics of bulk excitons at $T_b \leqslant T_c$ (T_c is the critical temperature for Bose-Einstein condensation of excitons in bulk semiconductors), similar to this case it depends only on two control parameters of the system, T_0 and T_b. Furthermore, the only gross information from a particular shape of the initial distribution at $t=0$ is absorbed by the start time t_c of the adiabatic stage of thermalization. This is shown in Fig. 1(a), where we vary the parameters of the initial Gaussian distribution. In turn, the first transient depends upon initial distribution and lasts only for a few scattering times τ_{sc}, as illustrated in Fig. 1(b).

Because at any nonzero bath temperature $T_b>0$ the occupation number of the ground-state mode $N^0_{\mathbf{k}_\parallel=\mathbf{0}}=\exp(T_0/T_b)-1$ is finite, the adiabatic stage ends up with linearized kinetics. The latter kinetics refers to the last, exponential stage of thermalization at $t\to\infty$ and is characterized by $N_{\mathbf{k}_\parallel=\mathbf{0}}(t)-N^0{}_{\mathbf{k}_\parallel=\mathbf{0}}\propto T(t)-T_b\propto e^{-\lambda_0 t}$. For statistically degenerate QW excitons, the thermalization time $\tau_{th}=1/\lambda_0(T_b,T_0)$ reaches its smallest values at bath temperatures $E_0/k_B \ll T_b \lesssim T_0$. While the above inequality does not usually hold in the experiments with statistically degenerate indirect excitons in GaAs/Al_xGa_{1-x}As-coupled QW's,[14–16,18–20] we describe a special design of GaAs-based microcavities (MC's) for optimization of the LA-phonon-assisted thermalization kinetics of low-density MC polaritons. In the proposed microcavities with a large positive detuning between the cavity and QW exciton modes, the MC polaritons have radiative lifetimes on a 100 ps–1 ns time scale, so that the phonon-assisted relaxation towards well-developed Bose-Einstein statistics with large occupation numbers can optically be visualized. Thus, the MC design we discuss is an interesting alternative to the semiconductor microcavities with zero detuning between the cavity mode and QW excitons (see, e.g., Ref. 36), where huge nonclassical occupation numbers of the low-energy MC polariton states have recently been observed.[37–42]

In numerical evaluations we use $M_x=0.21m_0$, $v_s=3.7\times10^5$ cm/s, and $D_x=15.5$ eV, relevant to GaAs/Al_xGa_{1-x}As-coupled QW's, and $M_x=0.86m_0$, $v_s=4.1\times10^5$ cm/s, and $D_x=6.9$ eV, relevant to single ZnSe QW's, respectively (m_0 is the free electron mass). Note that the disorder-induced scattering and localization processes, not included in our model, are relatively strong in up-to-date ZnSe-based QW's and require a separate analysis.[2,43] However, in a very recent work[44] the first fabrication of high-quality MgS/ZnSe/MgS QW's with less than 1 ML fluctuations of the well width and, therefore, with extremely low inhomogeneous broadening has been reported.

In Sec. II, the Boltzmann equation is adapted in order to formulate the acoustic-phonon-assisted kinetics of statistically degenerate QW excitons. We also discuss some approximations for the form factor $F_z(\chi)$, which describe the relaxation of momentum conservation in scattering of QW excitons by bulk LA phonons.

In Sec. III, we find the generic solution of the acoustic-phonon-assisted kinetics from a strongly nonequilibrium initial distribution of QW excitons $N_\varepsilon(t=0)$ towards a final Bose-Einstein distribution N^0_ε with large occupation numbers of the low-energy states, $N^0_{\varepsilon\simeq0}\gtrsim1$, where ε is the dimensionless energy defined by $\varepsilon=\hbar^2\mathbf{k}_\parallel^2/(2M_xE_0)$. The generic solution is independent of a particular shape of the initial distribution and describes the adiabatic stage of thermalization, which starts at $t=t_c$ with in a few characteristic scattering times after $t=0$. We show that at $t\gg t_c$ thermalization of high-energy QW excitons is given by $\delta T(t)\propto e^{-\lambda_0 t}/t$, where λ_0 is the lowest positive eigenvalue of the relevant linearized kinetics.

In Sec. IV, the linearized phonon-assisted kinetics of statistically degenerate QW excitons is formulated and analyzed. We show that the eigenvalues $\{\lambda\}$ of the linear collision integral form a continuous spectrum, $\infty>\lambda\geqslant\lambda_0>0$, separated from the nondegenerate eigenvalue $\lambda=0$, and that the corresponding eigenfunctions $\{\psi_\varepsilon(\lambda)\}$ have three well-defined isolated critical points. The dependence of the marginal eigenvalue λ_0 on the bath (T_b) and degeneracy (T_0) temperatures is studied.

In Sec. V, straightforward numerical simulations of the phonon-assisted relaxation kinetics at $T_b\lesssim T_0$ are compared with the generic solution of the quantum Boltzmann equation. We also show that at the beginning of the adiabatic stage of thermalization, at $t_c\leqslant t\lesssim\lambda_0^{-1}$, the population dynamics of the ground-state mode is given by $N_{\varepsilon=0}(t)\propto(1+\chi t)^\nu$, where the parameters χ and ν are calculated analytically. Furthermore, we propose a particular design of GaAs-based MC's, which compromises the efficiency of LA-phonon-assisted scattering (the density of states is $\propto M_x$) with the degeneracy temperature $T_0\propto M_x^{-1}$, i.e., allows us to avoid the bottleneck effect in relaxation and, therefore, to optimize the thermalization kinetics of low-density QW excitons.

In the Appendix, some relationships relevant to the thermalization dynamics of quasiequilibrated high-energy QW excitons are given.

II. BOLTZMANN KINETIC EQUATION FOR DEGENERATE QW EXCITONS

For hot QW excitons, which are in-plane isotropically distributed at $t=0$, the thermalization kinetics due to bulk LA phonons can be treated in one-dimensional energy space [see Eq. (2) of Ref. 10]. In the following we express energy E and temperature T (as well as T_b and T_0) in terms of E_0, i.e., we use the dimensionless values of $E\to\varepsilon=E/E_0$ and $T\to(k_BT)/E_0$. In order to derive and analyze the generic solution for relaxation at $T_b<T_0$, it is convenient to rewrite the above equation in terms of the variable

$$f_\varepsilon(t)=\frac{N_\varepsilon(t)-N^0_\varepsilon}{T_b(N^0_\varepsilon)'}, \tag{2.1}$$

where $N_\varepsilon(t)$ and $N^0_\varepsilon=1/[e^{(\varepsilon-\mu)/T_b}-1]$ are the current and (final) equilibrium distribution functions of QW excitons, re-

spectively, and the chemical potential μ is given by $\mu = T_b \ln(1-e^{-T_0/T_b})$. In this case the kinetic equation reduces to

$$\frac{\partial}{\partial t} f_\varepsilon(t) = -\frac{4}{\tau_{sc}}\left[\int_0^{\theta_S(\varepsilon)} F_S(\varepsilon,\varepsilon_1)\mathcal{L}_S(\varepsilon,\varepsilon_1,t)\varepsilon_1 d\varepsilon_1 + \int_{\theta_{AS}(\varepsilon)}^{\infty} F_{AS}(\varepsilon,\varepsilon_1)\mathcal{L}_{AS}(\varepsilon,\varepsilon_1,t)\varepsilon_1 d\varepsilon_1\right], \tag{2.2}$$

where the Stokes (S) and anti-Stokes (AS) collision integrands are

$$\mathcal{L}_S(\varepsilon,\varepsilon_1,t) = [f_\varepsilon(t) - f_{\varepsilon-\varepsilon_1}(t)](1+n^{ph}_{\varepsilon_1}+N^0_{\varepsilon-\varepsilon_1}) + T_b(N^0_{\varepsilon-\varepsilon_1})' f_\varepsilon(t) f_{\varepsilon-\varepsilon_1}(t), \tag{2.3a}$$

$$\mathcal{L}_{AS}(\varepsilon,\varepsilon_1,t) = [f_\varepsilon(t) - f_{\varepsilon+\varepsilon_1}(t)](n^{ph}_{\varepsilon_1}-N^0_{\varepsilon+\varepsilon_1}) - T_b(N^0_{\varepsilon+\varepsilon_1})' f_\varepsilon(t) f_{\varepsilon+\varepsilon_1}(t). \tag{2.3b}$$

The distribution of thermal bulk phonons is given by the Planck formula, i.e., $n^{ph}_\varepsilon = 1/(e^{\varepsilon/T_b}-1)$. The scattering time is defined by $\tau_{sc} = (\pi^2\hbar^4\rho)/(D_x^2 M_x^3 v_s)$. The functions $\theta_{S/AS}(\varepsilon)$, which determine the integration limits on the right-hand side of Eq. (2.2), are

$$\theta_S(\varepsilon) = \begin{cases} 0, & \varepsilon \leqslant 1/4 \\ 2\sqrt{\varepsilon}-1, & 1/4 < \varepsilon \leqslant 1 \\ \varepsilon, & 1 < \varepsilon, \end{cases} \tag{2.4a}$$

$$\theta_{AS}(\varepsilon) = \begin{cases} 1-2\sqrt{\varepsilon}, & \varepsilon \leqslant 1/4 \\ 0, & \varepsilon > 1/4. \end{cases} \tag{2.4b}$$

The functions $F_{S/AS}(\varepsilon,\varepsilon_1)$ in Eq. (2.2) are given by

$$F_{S/AS}(\varepsilon,\varepsilon_1) = \int_{d^{S/AS}_{\varepsilon,\varepsilon_1}}^{u^{S/AS}_{\varepsilon,\varepsilon_1}} |F_z(a\varepsilon_1\alpha)|^2 \{[(u^{S/AS}_{\varepsilon,\varepsilon_1})^2-\alpha^2] \times [\alpha^2-(d^{S/AS}_{\varepsilon,\varepsilon_1})^2]\}^{-1/2} d\alpha, \tag{2.5}$$

where $u^{S/AS}_{\varepsilon,\varepsilon_1} = [1-(\sqrt{\varepsilon}-\sqrt{\varepsilon \mp \varepsilon_1})^2/\varepsilon_1^2]^{1/2}$ and $d^{S/AS}_{\varepsilon,\varepsilon_1} = [1-(\sqrt{\varepsilon}+\sqrt{\varepsilon \mp \varepsilon_1})^2/\varepsilon_1^2]^{1/2}$. The dimensionless parameter a in the argument of the form factor function F_z is given by $a = (L_z M_x v_s)/\hbar$.

In order to estimate the contribution of the form factor $F_z(\chi)$ to the spectral functions $F_{S/AS}(\varepsilon,\varepsilon_1)$ one can analyze Eq. (2.5) for $\varepsilon \to 0$. In this case only the spectral function $F_{AS}(\varepsilon,\varepsilon_1)$ is relevant to the kinetic Eq. (2.2), and Equation (2.5) yields

$$F_{AS}(0,\varepsilon_1) = \frac{\pi}{2}\sqrt{\frac{\varepsilon_1}{\varepsilon_1-1}}|F_z[a\sqrt{\varepsilon_1(\varepsilon_1-1)}]|^2. \tag{2.6}$$

For $\varepsilon_1 \gg 1$, the spectral width $\Delta\varepsilon$ (full width at half maximum) of $F_{AS}(0,\varepsilon_1)$ is given, by $\Delta\varepsilon \simeq 2.26/a$ and determined solely by $F_z(a\varepsilon_1)$. For thickness $L_z = 8$ nm of GaAs QW's (see Ref. 18) one gets $a \simeq 0.054$ and, therefore, $\Delta\varepsilon \simeq 42$. The latter estimate can be rewritten in the dimensional energy units as $\Delta E = E_0 \Delta\varepsilon = 4.52\hbar v_s/L_z \simeq 1.44$ meV. Thus the spectral band of LA phonons, which scatter a low-energy QW exciton, can be evaluated as $\Delta E \sim v_s \Delta p_z$, where $\Delta p_z \sim \hbar/L_z$ is the uncertainty of the momentum in the z direction due to the QW spatial confinement. The above estimates show that for relatively cold QW excitons with energies $\varepsilon \leqslant \Delta\varepsilon$ (the effective temperature $T^{eff} = \Delta E/k_B \simeq 16.5$ K for $L_z = 8$ nm) the form factor can be approximated by $F_z(a\varepsilon_1\alpha) = F_z(0) = 1$. In this case the integral on the rhs of Eq. (2.5) can be calculated explicitly,

$$F_{S/AS}(\varepsilon,\varepsilon_1) = \frac{1}{d^{S/AS}_{\varepsilon,\varepsilon_1}}\Phi\left[\left(\frac{d^{S/AS}_{\varepsilon,\varepsilon_1}}{u^{S/AS}_{\varepsilon,\varepsilon_1}}\right)^2\right], \tag{2.7}$$

where

$$\Phi(\xi) = \begin{cases} -i\left\{F\left[\arcsin(\sqrt{\xi}), \frac{1}{\xi}\right] - K\left(\frac{1}{\xi}\right)\right\}, & 0 \leqslant \xi < 1 \\ K\left(\frac{1}{\xi}\right), & \xi < 0. \end{cases} \tag{2.8}$$

Here, $F(\phi,m) = \int_0^\phi [1-m\sin^2(\theta)]^{-1/2} d\theta$ and $K(m) = F(\pi/2,m)$ are the elliptic and the complete elliptic integrals of the first kind, respectively. Because in the analyzed case the relaxation kinetics depends only on $F_z(0)$, the functions $F_{S/AS}(\varepsilon,\varepsilon_1)$ can easily be rescaled for any particular shape of the QW confinement potential.

III. GENERIC SOLUTION

In this section the thermalization kinetics at $T_b \leqslant T_0$ is described in terms of a generic solution, which weakly correlates with the initial distribution $N_\varepsilon(t=0)$. In particular, we derive a thermalization law for high-energy excitons and examine nonequilibrium distribution of low-energy QW excitons. We also specify a reference point for the generic solution, i.e., a set of parameters, which unambiguously determines the calculated evolution. Schematic picture of the relaxation kinetics in phase space is shown in Fig. 2. The generic solution is relevant to the times $t > t_c$, where t_c is the start time of the adiabatic stage of evolution.

As was emphasized in Sec. I, the generic solution assumes a quasiequilibrium distribution of *high-energy* excitons ($\varepsilon > 1/4$): $N_{\varepsilon>1/4}(t) = 1/[\exp([\varepsilon-\tilde{\mu}(t)]/T(t))-1]$. This quasiequilibrium distribution is characterized by the effective time-dependent temperature $T(t) = T_b + \delta T(t)$ and chemical potential $\tilde{\mu}(t)$ whose time variations are supposed to be small, so that $\tilde{\mu}(t)$ can be taken the same as the chemical potential of final equilibrium distribution $\tilde{\mu}(t) \simeq \mu$. Indeed, for $T(t) < T_0$ the chemical potential is given by $\tilde{\mu}(t) \simeq -T(t)e^{-T_0/T(t)} \ll T(t)$ and, therefore, $|\delta\mu| = |\tilde{\mu}(t)-\mu|$

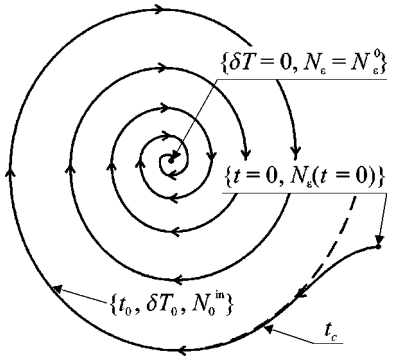

FIG. 2. Schematic picture of the relaxation kinetics at $T_b \lesssim T_0$. The reference (start) point $\{t_0, \delta T_0, N_0^{\rm in}\}$ unambiguously determines the calculated (solid line) evolution from the initial nonequilibrium distribution $N_\varepsilon(t=0)$. The dashed line corresponds to the generic solution. t_c is the start point of adiabatic stage of evolution. For the times $t-t_c \geqslant \tau_{\rm sc}$ both evolution spirals almost coincide showing a unique path towards the final equilibrium distribution $\{\delta T=0, N_\varepsilon = N_\varepsilon^0\}$.

$\ll \delta T(t)$. Since at the final stage of relaxation kinetics the effective temperature of high-energy excitons approaches the bath temperature $[\delta T(t) \to 0]$, starting from some moment in time one meets the condition $\delta T(t) \ll T_b$ (provided that $T_b > 0$). Therefore we can linearize the quasiequilibrium distribution function with respect to $\delta T(t)$. In this case one obtains

$$f_{\varepsilon > 1/4}(t) = -[\delta T(t)/T_b^2]\varepsilon. \tag{3.1}$$

On the other hand, as we show below, a *low-energy* kernel $(0 < \varepsilon \leqslant 1/4)$ of the distribution function characterizes the nonequilibrium QW excitons. With increasing time $t \geqslant t_c$, the low-energy kernel shrinks in energy space and the ratio $|N_{\varepsilon \leqslant 1/4} - N^0_{\varepsilon \leqslant 1/4}|/N^0_{\varepsilon \leqslant 1/4}$ decreases approaching the limit when the linearized kinetics becomes valid.

A. Nonequilibrium distribution of low-energy QW excitons

In order to analyze the evolution of low-energy QW excitons within the scenario described in the preceding section, we substitute Eq. (3.1) into Eq. (2.2) and get the reduced kinetic equation for $\varepsilon \leqslant 1/4$,

$$\frac{\partial}{\partial t} f_\varepsilon(t) = -[\xi_0(\varepsilon) + \xi_1(\varepsilon)\delta T(t)] f_\varepsilon(t) + \eta(\varepsilon)\delta T(t), \tag{3.2}$$

where

$$\xi_0(\varepsilon) = \frac{4}{\tau_{\rm sc}} \int_{1-2\sqrt{\varepsilon}}^{\infty} F_{\rm AS}(\varepsilon, \varepsilon_1)(n^{\rm ph}_{\varepsilon_1} - N^0_{\varepsilon+\varepsilon_1})\varepsilon_1 d\varepsilon_1, \tag{3.3}$$

$$\xi_1(\varepsilon) = \frac{4}{\tau_{\rm sc} T_b} \int_{1-2\sqrt{\varepsilon}}^{\infty} F_{\rm AS}(\varepsilon, \varepsilon_1)(N^0_{\varepsilon+\varepsilon_1})' \varepsilon_1(\varepsilon+\varepsilon_1) d\varepsilon_1, \tag{3.4}$$

$$\eta(\varepsilon) = -\frac{4}{\tau_{\rm sc} T_b^2} \int_{1-2\sqrt{\varepsilon}}^{\infty} F_{\rm AS}(\varepsilon, \varepsilon_1)(n^{\rm ph}_{\varepsilon_1} - N^0_{\varepsilon+\varepsilon_1}) \times \varepsilon_1(\varepsilon+\varepsilon_1) d\varepsilon_1, \tag{3.5}$$

and $F_{\rm AS}(\varepsilon+\varepsilon_1)$ is given by Eq. (2.7). Equation (3.2), which describes the population dynamics of the low-energy states during the adiabatic stage of thermalization $(t \geqslant t_c)$, is a linear inhomogeneous differential equation for $f_{\varepsilon \leqslant 1/4}$. Its complete solution can be written as a sum of the homogeneous and inhomogeneous contributions,

$$f_{\varepsilon \leqslant 1/4}(t) = f^{\rm hom}_{\varepsilon \leqslant 1/4}(t) + \eta(\varepsilon) \int_{t_0}^{t} \exp[-(t-\tau)\xi_0(\varepsilon) - \rho(t,\tau)\xi_1(\varepsilon)]\delta T(\tau) d\tau, \tag{3.6}$$

where

$$f^{\rm hom}_{\varepsilon \leqslant 1/4}(t) = \exp[-(t-t_0)\xi_0(\varepsilon) - \rho(t,t_0)\xi_1(\varepsilon)] \times f_{\varepsilon \leqslant 1/4}(t=t_0), \tag{3.7}$$

$$\rho(t,t_1) = \int_{t_1}^{t} \delta T(\tau) d\tau, \tag{3.8}$$

and t_0 is an arbitrary reference (start) time for the calculated evolution, i.e., $t_0 \geqslant t_c$ (see Fig. 2).

Thus the adiabatic stage of the relaxation kinetics into the lower-energy states is completely determined by $N_\varepsilon(t) = N^0_\varepsilon + T_b (N^0_\varepsilon)' f_\varepsilon(t)$, provided that one knows the reference (start) distribution $f_{\varepsilon \leqslant 1/4}(t=t_0)$ and thermalization law $\delta T = \delta T(t)$ for high-energy QW excitons. Note that in a sharp contrast with the acoustic-phonon-assisted relaxation kinetics at $T_b \leqslant T_c$ in three-dimensional systems,[45] the thermalization dynamics of low-energy QW excitons depends upon the homogeneous contribution $f^{\rm hom}_{\varepsilon \leqslant 1/4}$ given by Eq. (3.7).

As will be shown in the following section, the thermalization law for quasiequilibrium high-energy QW excitons $(\varepsilon > 1/4)$ is given by

$$\delta T(t) = \left(\frac{\delta T_0}{\lambda_1 - \lambda_0}\right) \frac{e^{-\lambda_0(t-t_0)} - e^{-\lambda_1(t-t_0)}}{t-t_0}, \tag{3.9}$$

where $\lambda_0 = \xi_0(0)$ characterizes the inverse thermalization time at $t \to \infty$, $\lambda_1 = \xi_0(1/4)$ is another characteristic parameter relevant to the beginning of the adiabatic stage $(\lambda_1 \gg \lambda_0)$, and $\delta T_0 = \delta T(t=t_0)$ determines reference (start) effective temperature $T(t=t_0) = T_b + \delta T_0$ for the calculated evolution. Equation (3.9) is valid for $t \geqslant t_0$. Using the thermalization law (3.9) we find the integral on the rhs of Eq. (3.8),

$$\rho(t,t_1) = \frac{\delta T_0}{\lambda_1 - \lambda_0}\{{\rm Ei}[-\lambda_0(t-t_0)] - {\rm Ei}[-\lambda_0(t_1-t_0)] - {\rm Ei}[-\lambda_1(t-t_0)] + {\rm Ei}[-\lambda_1(t_1-t_0)]\}, \tag{3.10}$$

where ${\rm Ei}(z) = -\int_{-z}^{\infty}(e^{-t}/t)dt$ is the exponential integral function.

The reference distribution $f_{\varepsilon\leqslant 1/4}(t=t_0)$, which determines the homogeneous solution (3.7), is independent of the initial distribution of hot QW excitons, $N_\varepsilon(t=0)$. There is, however, an integral relationship between δT_0 and $f_{\varepsilon\leqslant 1/4}(t=t_0)$, which we will discuss in Sec. III C along with possible approximations for $f_{\varepsilon\leqslant 1/4}(t=t_0)$.

B. Thermalization of high-energy QW excitons

The temperature change $\delta T=\delta T(t)$ characterizes the time evolution of high-energy quasiequilibrated particles through Eqs. (2.1) and (3.1). In order to derive the temperature law (3.9) we substitute $f_{\varepsilon\leqslant 1/4}$ and $f_{\varepsilon>1/4}$ given by Eqs. (3.6) and (3.1), respectively, into the kinetic equation (2.2),

$$\frac{\partial}{\partial t}\delta T(t)=-[\alpha_0+\alpha_1(t)]\delta T(t)+\beta\delta T^2(t)+\gamma(t), \tag{3.11}$$

where

$$\gamma(t)=-\frac{4T_b^2}{\tau_{\rm sc}\varepsilon_c}\int_0^{1/4}F_{\rm S}(\varepsilon_c,\varepsilon_c-\varepsilon)(1+n^{\rm ph}_{\varepsilon_c-\varepsilon}N^0_\varepsilon)\times f_\varepsilon(t)(\varepsilon_c-\varepsilon)d\varepsilon, \tag{3.12}$$

and the parameters α_0,β, and functional $\alpha_1(t)=\alpha_1[f_{\varepsilon\leqslant 1/4}(t)]$ are defined in the Appendix. Equations (3.11) and (3.12) refer to some energy $\varepsilon_c\gtrsim 1$ from the high-energy domain $\varepsilon>1/4$.

In the adiabatic stage of relaxation, when $t>t_c$, one has $\delta T(t)/T_b\ll 1$ so that α_1 and $\beta\delta T^2$ can be neglected on the rhs of Eq. (3.11), because $|\alpha_1(t)|\ll\alpha_0$ and $|\beta\delta T^2(t)|\ll|\gamma(t)|$. At the end of the adiabatic stage ($t-t_c\gg\lambda_0^{-1}$) the distribution function $N_\varepsilon(t)$ is already very close to N^0_ε even for small energies $\varepsilon\leqslant 1/4$ and, therefore, the phonon-assisted relaxation kinetics becomes exponential, i.e., $\delta T(t)\propto e^{-\lambda_0 t}$. For statistically degenerate QW excitons ($N^0_{\varepsilon=0}\gg 1$) one estimates from Eqs. (3.3) and (A1) that positive $\lambda_0=\xi(0)$ is much less than positive α_0. In this case Eq. (3.11) can be solved iteratively. The first iteration, which can formally be obtained by neglecting the time derivative on the rhs of Eq. (3.11), yields

$$\delta T(t)=\gamma(t)/\alpha_0. \tag{3.13}$$

For the same time domain $t-t_c\gg\lambda_0^{-1}$ Eq. (3.6) yields the following approximation:

$$f_{\varepsilon\leqslant 1/4}(t)=\exp[-(t-t_0)\xi_0(\varepsilon)]f_\varepsilon(t=t_0)+\frac{\eta(\varepsilon)}{\xi_0(\varepsilon)}\delta T(t). \tag{3.14}$$

By substituting Eq. (3.14) into the rhs of Eq. (3.12) one derives from Eq. (3.13)

$$\delta T(t)=\frac{1}{\tilde{\alpha}}\int_0^{1/4}F_{\rm S}(\varepsilon_c,\varepsilon_c-\varepsilon)(1+n^{\rm ph}_{\varepsilon_c-\varepsilon}N^0_\varepsilon)f_\varepsilon(t_0)\times\exp[-(t-t_0)\xi_0(\varepsilon)](\varepsilon_c-\varepsilon)d\varepsilon, \tag{3.15}$$

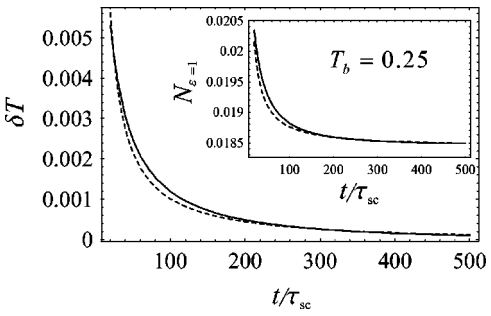

FIG. 3. Time dependence of δT and $N_{\varepsilon=1}$ (inset) calculated by using the thermalization law (3.9) (dashed lines) and by direct numerical modeling of the initial kinetic equation (2.2) (solid lines). The control parameters T_b and T_0 are the same as in Fig. 1.

where the constant $\tilde{\alpha}$ is defined in the Appendix. We can further simplify Eq. (3.15) taking into account that $\xi_0(\varepsilon)$ is a monotonically increasing function of energy and that at large t only the small vicinity of $\varepsilon=0$ contributes to the integral. Finally, we end up with the asymptotic law

$$\delta T(t)=\left(\frac{\tilde{\gamma}_0}{\tilde{\alpha}}\right)\frac{\exp[-\xi_0(0)(t-t_0)]-\exp[-\xi_0(1/4)(t-t_0)]}{t-t_0}, \tag{3.16}$$

where the constant $\tilde{\gamma}_0$ is given in the Appendix. Equation (3.16) is identical to Eq. (3.9) provided that the reference (start) temperature $T_b+\delta T(t=t_0)$ of the high-energy quasiequilibrated QW excitons is determined by

$$\delta T_0\equiv\delta T(t=t_0)=(\tilde{\gamma}_0/\tilde{\alpha})(\lambda_1-\lambda_0). \tag{3.17}$$

While the above derivation of Eqs. (3.13)–(3.17) assumes that $t-t_c\gtrsim t-t_0\gg\lambda_0^{-1}$, we have checked numerically that *the temperature law* (3.9) *holds through the whole adiabatic stage*, i.e., for the time interval $0\leqslant t-t_0<\infty$. Furthermore, the numerical evaluations also clearly indicate that the start temperature $\delta T(t=t_0)$ is practically independent of the local energy $\varepsilon_c\gtrsim 1$ used in the derivation of Eqs. (3.11)–(3.17). In Fig. 3 we plot $\delta T=\delta T(t)$ and $N_{\varepsilon=1}=N_{\varepsilon=1}(t)$ calculated by using the thermalization law (3.9) (dashed lines) and by direct numerical modeling of the initial kinetic equation (2.2) (solid lines), respectively.

For the time domain $\lambda_1^{-1}\leqslant t-t_0\leqslant\lambda_0^{-1}$ the thermalization law (3.9) can be approximated by $\delta T(t)=(\lambda_1-\lambda_0)^{-1}\delta T_0/(t-t_0)$. The latter dependence $\delta T(t)\propto 1/(t-t_0)$ is consistent with that found for the adiabatic stage of the phonon-assisted relaxation kinetics of 3D bosons (excitons) at $T_b\leqslant T_c$, when the Bose-Einstein condensate builds up.[45] For 2D systems at nonzero T_b the occupation number of the ground-state mode $N^0_{\varepsilon=0}$ is always final. Therefore the exponential kinetics $\delta T(t)\propto e^{-\lambda_0(t-t_0)}$, which results from Eq. (3.9) for $t-t_0\gtrsim\lambda_0^{-1}$, develops at the final stage of relaxation, when $|N_{\varepsilon=0}(t)-N^0_{\varepsilon=0}|/N^0_{\varepsilon=0}\ll 1$. Note that because for statistically degenerate QW excitons, when $T_b\leqslant T_0$ and $N^0_{\varepsilon=0}\gg 1$, one has $\lambda_0^{-1}\gg\tau_{sc}$ (see Sec. IV), the two modes of behavior, $\delta T\propto 1/t$ and $\delta T\propto e^{-\lambda_0 t}$, are well-separated in time.

C. Reference point for the generic solution

In order to determine the relaxation kinetics of low-energy particles, i.e., $N_{\varepsilon\leqslant 1/4}=N_{\varepsilon\leqslant 1/4}(t\geqslant t_c)$, one needs to specify the reference distribution $f_{\varepsilon\leqslant 1/4}(t=t_0)$ and $\delta T_0=\delta T(t=t_0)=T(t=t_0)-T_b$. According to Eq. (3.7), with increasing time $t-t_0$ only the small vicinity of $\varepsilon=0$ gives contributes to the homogeneous part of the generic solution. Therefore we approximate $N_{\varepsilon\leqslant 1/4}(t=t_0)\simeq N_0^{\rm in}\equiv N_{\varepsilon=0}(t=t_0)$. The above approximation assumes that the reference time $t_0\geqslant t_c$ is close enough to the start time t_c of the adiabatic stage of relaxation so that $N_\varepsilon(t_0)\ll N_\varepsilon^0$ at $\varepsilon\ll 1/4$. Thus, using Eq. (2.1) we determine the reference distribution at $t=t_0$ by

$$f_{\varepsilon\leqslant 1/4}(t=t_0)=\frac{N_0^{\rm in}-N_\varepsilon^0}{T_b(N_\varepsilon^0)'}. \tag{3.18}$$

The latter expression is completely defined by the only one unknown parameter $N_0^{\rm in}$, the population of the ground-state mode at the reference time t_0.

Equation (3.18) allows us to find $\delta T_0=\delta T(t=t_0)$ through the integral relationship (3.15) taken at $t=t_0$. Furthermore, within the approximations used in the derivation of the asymptotic law (3.16) a simplified (algebraic) form of this relationship, given by Eqs. (3.17) and (A5), is valid as well. After the value of δT_0 is determined, using the thermalization law (3.9) one can easily find the time dependence of the distribution function (3.1) of high-energy excitons. Therefore, the three parameters t_0, $N_0^{\rm in}$, and δT_0, completely specify the reference point for the generic solution, as illustrated in Fig. 2.

IV. LINEARIZED KINETICS FOR STATISTICALLY DEGENERATE QW EXCITONS

If for any energy ε the distribution function N_ε of quantum-degenerate quasi-2D excitons is close enough to final N_ε^0 so that $|N_\varepsilon-N_\varepsilon^0|/N_\varepsilon^0\ll 1$ and $f_\varepsilon(t)$ becomes small, the phonon-assisted kinetics can be linearized. In particular, the adiabatic stage of thermalization at times $t-t_0\geqslant\lambda_0^{-1}$ refers to the linearized kinetics. The linearized kinetics can be described in terms of the real eigenvalues $\{\lambda\}(\lambda\geqslant 0)$ and the corresponding eigenfunctions $\{\psi_\varepsilon(\lambda)\}$ so that $f_\varepsilon(t)=\Sigma_\lambda c_\lambda\psi_\varepsilon(\lambda)\exp(-\lambda t)$. The initial kinetic equation (2.2) reduces to the linear Fredholm equation of the second kind with respect to $\psi_\varepsilon(\lambda)$,

$$\lambda\psi_\varepsilon(\lambda)=\frac{4}{\tau_{\rm sc}}\left[\int_0^{\theta_{\rm S}(\varepsilon)}F_{\rm S}(\varepsilon,\varepsilon_1)\tilde{\mathcal{L}}_{\rm S}(\varepsilon,\varepsilon_1)\varepsilon_1 d\varepsilon_1+\int_{\theta_{\rm AS}(\varepsilon)}^{\infty}F_{\rm AS}(\varepsilon,\varepsilon_1)\tilde{\mathcal{L}}_{\rm AS}(\varepsilon,\varepsilon_1)\varepsilon_1 d\varepsilon_1\right], \tag{4.1}$$

where

$$\tilde{\mathcal{L}}_{\rm S}(\varepsilon,\varepsilon_1)=[\psi_\varepsilon(\lambda)-\psi_{\varepsilon-\varepsilon_1}(\lambda)](1+n_{\varepsilon_1}^{\rm ph}+N_{\varepsilon-\varepsilon_1}^0), \tag{4.2a}$$

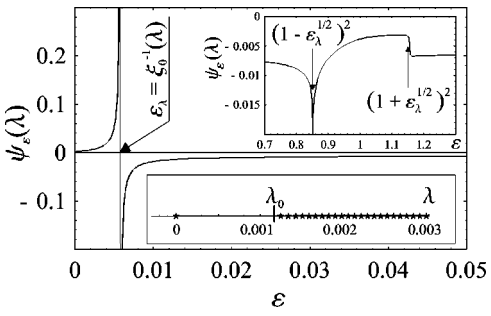

FIG. 4. A typical shape of the eigenfunction $\psi_\varepsilon(\lambda)$. The main part of the figure shows the first-order pole, which arises at the energy region $\varepsilon<1/4(\lambda=0.0043/\tau_{\rm sc}$ in this particular example). The top inset illustrates eigenfunction behavior at critical points in the high-energy band $\varepsilon\geqslant 1$. The eigenvalue spectrum (λ in units $1/\tau_{\rm sc}$) is shown in the bottom inset. The control parameters T_b and T_0 are the same as in Fig. 1.

$$\tilde{\mathcal{L}}_{\rm AS}(\varepsilon,\varepsilon_1)=[\psi_\varepsilon(\lambda)-\psi_{\varepsilon+\varepsilon_1}(\lambda)](n_{\varepsilon_1}^{\rm ph}-N_{\varepsilon+\varepsilon_1}^0), \tag{4.2b}$$

and functions $\theta_{\rm S}$ and $\theta_{\rm AS}$ are given by Eqs. (2.4a) and (2.4b), respectively.

Thus we replace the solution of Eq. (2.2) by the eigenfunction analysis of the Fredholm integral equation (4.1). The numerical solution of Eq. (4.1) clearly shows that for a given $T_b>0$ all eigenvalues $\{\lambda\}$ except one are nondegenerate, positive, and belong to the continuous spectrum. This is illustrated in the bottom inset of Fig. 4, where the set of eigenvalues shown by the stars covers the same interval $\infty>\lambda\geqslant\lambda_0=\lambda_0(T_b,T_0)$ and will be more dense if more discrete points in energy space are used. The isolated nondegenerate eigenvalue $\lambda=0$ is due to conservation of the total number of QW excitons in our model (the only integral of motion of the system[46]).

Since all $\{\lambda\}$ are nondegenerate, the corresponding eigenfunctions $\{\psi_\varepsilon(\lambda)\}$ form a basis in Hilbert energy space. For the energy band $0\leqslant\varepsilon<1/4$ one derives from Eq. (4.1),

$$\psi_{\varepsilon<1/4}(\lambda)=\frac{\sigma(\varepsilon)}{\lambda-\xi_0(\varepsilon)}, \tag{4.3}$$

where $\sigma(\varepsilon)$ is a smooth regular function of ε given by

$$\sigma(\varepsilon)=-\frac{4}{\tau_{\rm sc}}\int_0^{\theta_{\rm S}(\varepsilon)}F_{\rm S}(\varepsilon,\varepsilon_1)\psi_{\varepsilon+\varepsilon_1}(\lambda)(n_{\varepsilon_1}^{\rm ph}-N_{\varepsilon+\varepsilon_1}^0)\varepsilon_1 d\varepsilon_1, \tag{4.4}$$

and $\xi_0(\varepsilon)$ is defined by Eq. (3.3). Thus the eigenfunction $\psi_\varepsilon(\lambda)$ has an isolated singularity (first-order pole) at $\varepsilon_\lambda=\xi_0^{-1}(\lambda)$. The singularity is integrable in terms of principal-value integration. A typical shape of the eigenfunctions at $\varepsilon<1/4$ is shown in Fig. 4. In the energy band $\varepsilon\geqslant 1/4$ the eigenfunction has another singularity at the point $(1-\sqrt{\varepsilon_\lambda})^2$. This singularity is logarithmic, i.e., integrable. It arises when the singularity of $\psi_{\varepsilon-\varepsilon_1}(\lambda)$ at $\varepsilon-\varepsilon_1=\varepsilon_\lambda$ [see Eq. (4.2)] coincides with the upper boundary of integration, $\theta_{\rm S}(\varepsilon)$, in the Stokes collision term on the rhs of Eq. (4.1). The steplike jump at the critical point $(1+\sqrt{\varepsilon_\lambda})^2$ is not ac-

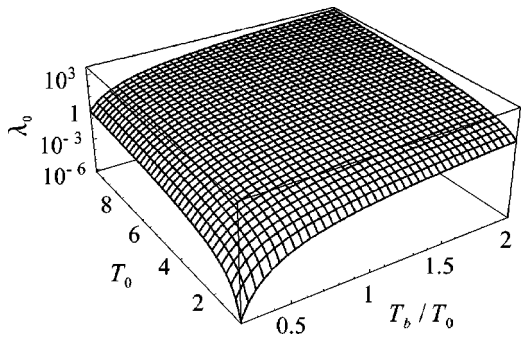

FIG. 5. The inverse thermalization time λ_0 (in units $1/\tau_{sc}$) as a function of the control parameters T_b and T_0.

companied by discontinuity of the eigenfunction. The latter critical point originates from a singular behavior of the form-factor function $F_S(\varepsilon,\varepsilon_1)$ at $\varepsilon_1=2\sqrt{\varepsilon}-1$. The features of the eigenfunction $\psi_\varepsilon(\lambda)$ at points $\varepsilon=(1\pm\sqrt{\varepsilon_\lambda})^2$ are shown in the top inset of Fig. 4.

The marginal point $\lambda_0=\lambda_0(T_b,T_0)$ of the continuous spectrum of $\{\lambda\}$ is indeed given by $\lambda_0=\xi_0(0)$: for $\lambda\to\lambda_0$ the singularity point $\varepsilon_\lambda\to 0$, i.e., it approaches its lowest limit. Because λ_0^{-1} is the longest relaxation time generated by the continuum $\lambda_0\leqslant\lambda<\infty$, the eigenavalue λ_0 determines the phonon-assisted kinetics at $t\to\infty$ and, in particular, yields the characteristic thermalization time in the relaxation thermodynamics developed in Ref. 10. The dependence of λ_0 upon the control parameters of the system, T_b and T_0, is plotted in the Fig. 5.

The eigenvalue λ_0 can reach both limits, i.e., $\lambda_0\gg\tau_{sc}^{-1}$ and $\lambda_0\ll\tau_{sc}^{-1}$ (see Fig. 5). The first limit, which corresponds to the considerable acceleration of the thermalization kinetics in comparison with that in the 3D case, is due to the relaxation of momentum conservation in QW exciton–bulk-acoustic-phonon scattering. The slowing down of thermalization, $\lambda_0\ll\tau_{sc}^{-1}$, occurs (i) at low bath temperatures $T_b\leqslant 1$, due to the exponentially decreasing number of thermal acoustic phonons with energy $\varepsilon\geqslant 1$, and/or (ii) for well-developed quantum statistics ($T_0\gg T_b$), due to an effective suppression of the stimulated kinetic processes. There is no direct phonon-mediated interaction of low-energy QW excitons $\varepsilon\leqslant 1/4$, and at low temperatures $T_b\leqslant 1$ the relaxation kinetics occurs by the two-step process: ''low-energy QW exciton ($\varepsilon\ll 1/4$) + phonon ($\varepsilon_1\simeq 1$)$\to$ QW exciton ($\varepsilon_2=\varepsilon+\varepsilon_1\simeq 1$) $\to$ low-energy QW exciton ($\varepsilon_4=\varepsilon+\varepsilon_1-\varepsilon_3\ll 1/4$)+ phonon ($\varepsilon_3\simeq 1$).'' The first, anti-Stokes transition quenches with decreasing temperature $T_b\leqslant 1$ and yields a temperature-dependent bottleneck effect in thermalization. In turn, the critical slowing down of the relaxation kinetics at $T_0\gg T_b$ arises due to mutual compensation of two stimulated fluxes, into and out the low-energy QW states $\varepsilon\ll 1$. For example, for the ground-state mode $\varepsilon=0$ the collision integrand responsible for the stimulated kinetics is given by $N_{\varepsilon=0}(N_{\varepsilon_1\geqslant 1}-n^{\rm ph}_{\varepsilon_1\geqslant 1})$. At $T_0\gg T_b$ the latter combination becomes small in spite of a large occupation number $N_{\varepsilon=0}\gg 1$, because $|N_{\varepsilon_1\geqslant 1}-n^{\rm ph}_{\varepsilon_1\geqslant 1}|\simeq|N^0_{\varepsilon_1\geqslant 1}-n^{\rm ph}_{\varepsilon_1\geqslant 1}|\to 0$ as a result of a very small value of the chemical potential, $|\mu|\ll 1$.

Now we can give an alternative proof of the temperature law (3.9), which refers to high-energy QW excitons with $\varepsilon>1/4$. Namely, the function $f_\varepsilon(t=t_0)$ can be expanded over the basis $\{\psi_\varepsilon(\lambda)\}$. Then the solution of Eq. (2.2) is given by

$$f_\varepsilon(t)=\int_{\lambda_0}^{\infty}c_\lambda\psi_\varepsilon(\lambda)e^{-\lambda(t-t_0)}d\lambda, \tag{4.5}$$

where c_λ are the expansion coefficients. At large times $t-t_0\gg\tau_{\rm th}$ only a small vicinity of λ near λ_0 contributes to the integral, due to the time exponent in the integrand. If now one assumes a regular distribution of quasi-2D excitons at $t=t_0$, the coefficients c_λ smoothly depend upon λ. As a result, the approximation $c_\lambda\simeq c_{\lambda_0}$ can be used in the integrand on the rhs of Eq. (4.5). Furthermore, the eigenfunctions $\psi_\varepsilon(\lambda)$ have nearly the same smooth shape at high energies as illustrated by Fig. 5. Thus we can also put $\psi_\varepsilon(\lambda)\simeq\psi_\varepsilon(\lambda_0)$ on the rhs of Eq. (4.5). As a result, both c_λ and $\psi_\varepsilon(\lambda)$ can be extracted out of the integral. Using Eq. (3.1) we immediately get $\delta T(t)\propto e^{-\lambda_0(t-t_0)}/(t-t_0)$, which coincides with Eq. (3.9) at $t-t_0\gg\lambda_1^{-1}$. Note that the above derivation is based on the particular spectrum ($\lambda=0+$ continuum $\lambda_0\leqslant\lambda<\infty$) of the linearized collision integral and has no analogy in the relaxation kinetics due to particle-particle interaction. In the latter case the fivefold degenerate eigenvalue $\lambda=0$ is separated from the continuous spectrum by a set of discrete isolated eigenvalues.[46]

V. DISCUSSION

In order to test the generic solutions (3.3)–(3.10) we model the phonon-assisted relaxation of excitons within the initial kinetic equation (1.1) reduced to energy space [Eqs. (2.1) and (2.2)]. An adaptive inhomogeneous grid with 100–200 points for ε is used to cover the close vicinity of the ground-state mode $\varepsilon=0$ (the maximum value of the dimensionless energy is $\varepsilon_{\rm max}=20$). Equation (2.2) is evaluated by a fourth-order Runge-Kutta integration routine with a time step of $(0.001-0.01)\tau_{sc}$. In order to calculate integrals on the rhs of Eq. (2.2) we perform a spline approximation for $f_\varepsilon(t)$ at every iterative step.

In numerical simulations we use the dimensionless temperatures T_b and T_0 and measure time in τ_{sc}. This makes our results suitable for various QW's and sets of the control parameters, provided that E_0 and τ_{sc} are specified. In Fig. 6 time evolution of the distribution $N_\varepsilon(t)=N^0_\varepsilon+T_b(N^0_\varepsilon)'f_\varepsilon(t)$ as a numerical solution of Eq. (2.2) is compared with the corresponding generic solution (3.3)–(3.10) relevant to $T_b<T_0$. All plots demonstrate an excellent agreement between analytical and numerical solutions. Note that at high T_b, e.g., $T_b=10$ (see the top plot in Fig. 6), the thermalization time $\tau_{\rm th}=\lambda_0^{-1}$ achieves the limit $\tau_{\rm th}\ll\tau_{sc}$, and the relative duration of the adiabatic stage estimated in terms of t_c (duration of the first transient) becomes smaller than that at $T_b\leqslant 1$. In this case the influence of the initial distribution $N_\varepsilon(t=0)$ slightly affects the calculated evolution at the beginning of the adiabatic stage, and the analytical solution fits to numerically simulated data become a little worse as can be seen for the distribution functions at $t=0.015\tau_{sc}$.

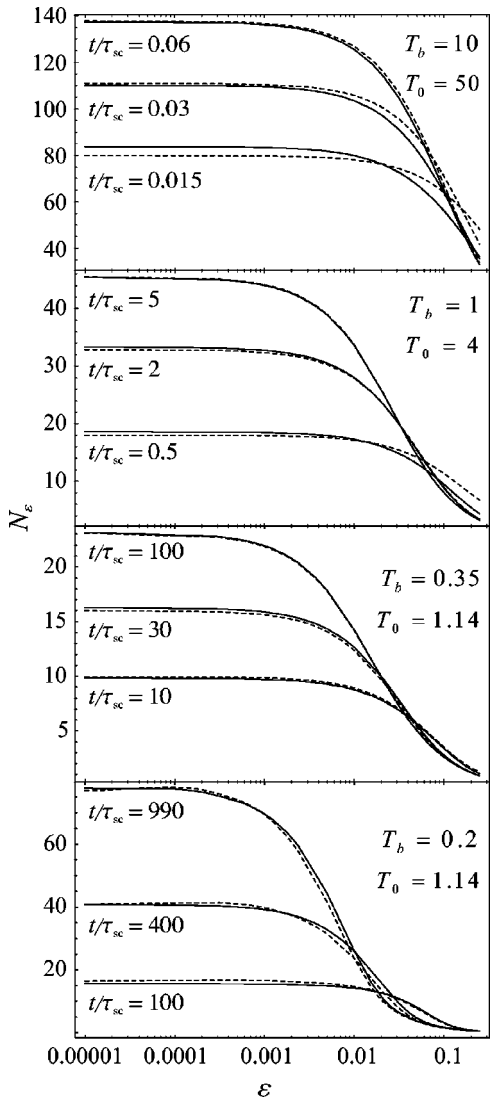

FIG. 6. Evolution of the distribution function N_ε at the adiabatic stage calculated for various sets of the control parameters T_b and T_0. Solid lines correspond to numerical evaluation of Eq. (2.2); dashed lines are obtained using the generic solution given by Eq. (3.6).

In contrast, at low T_b the relaxation kinetics at the adiabatic stage is slow. For example, at $T_b \leqslant 0.25$ it lasts for more than 1000 scattering times, where typical values of τ_{sc} in $GaAs/Al_xGa_{1-x}As$- coupled QW's are on a scale of tens of nanoseconds.

In Fig. 7 we also compare time dependences for the ground-state mode population $N_{\varepsilon=0}=N_{\varepsilon=0}(t)$ obtained numerically (solid lines) and analytically (dashed lines). Again, this figure shows that at $\varepsilon=0$ the generic solution (3.3)–(3.10) reproduces the adiabatic stage of the phonon-assisted relaxation kinetics very well. Within the time interval $0 \leqslant t-t_0 \lesssim \tau_{th}$ the generic solution yields the following simple approximation for the adiabatic kinetics into the ground-state mode:

$$N_{\varepsilon=0}(t)=N_0^{in}[1+\chi(t-t_0)]^\nu. \tag{5.1}$$

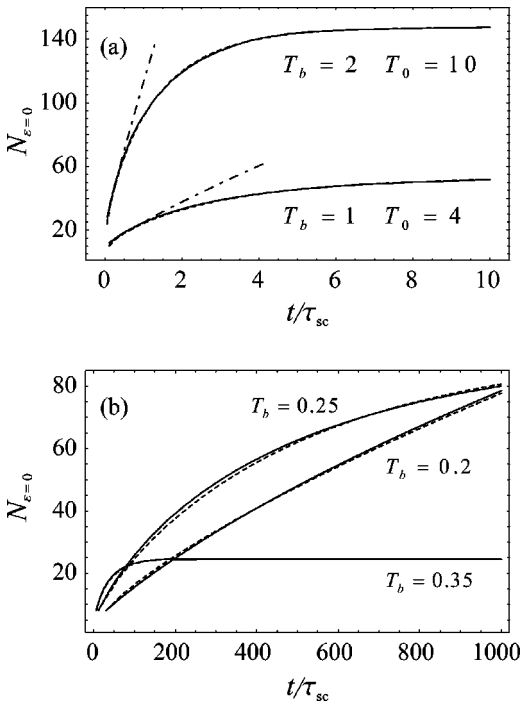

FIG. 7. Population dynamics of the ground-state mode $N_{\varepsilon=0}=N_{\varepsilon=0}(t)$ calculated for different bath temperatures at $T_0=4,10$ (a) and $T_0=1.14$ (b). Similarly to Fig. 6, the solid and dashed curves are calculated by using Eqs. (2.2) and (3.6), respectively. Dash-dotted lines correspond to time dependences $N_{\varepsilon=0}(t)$ calculated using approximate equation (5.1).

Parameters χ and ν can be found by comparing series expansions of Eqs. (5.1) and (3.6) about the point $t=t_0$. In such a way we get $\chi=(c_1^2-c_2N_0^{in})/(c_1N_0^{in})$ and $\nu=c_1^2/(c_1^2-c_2N_0^{in})$, where time-independent constants c_1 and c_2 are given by

$$c_1=(N^0_{\varepsilon=0}-N_0^{in})[\lambda_0+\delta T_0\xi_1(0)]+T_b\delta T_0\eta(0)(N^0_{\varepsilon=0})',$$

$$c_2=\frac{1}{2}((N_0^{in}-N^0_{\varepsilon=0})\{2\lambda_0^2+\delta T_0\xi_1(0) \times[5\lambda_0+\lambda_1+2\delta T_0\xi_1(0)]\}-T_b\delta T_0\eta(0)(N^0_{\varepsilon=0})' \times[3\lambda_0+\lambda_1+2\delta T_0\xi_1(0)]). \tag{5.2}$$

Time dependences of the ground-state-mode population $N_{\varepsilon=0}(t)$ calculated at $T_b=1$ and $T_b=2$ using Eq. (5.1) are shown in Fig. 7(a) with dash-dotted lines. At $t-t_0>\tau_{th}$ the approximation (5.1) is violated because the phonon-assisted relaxation kinetics starts to become exponential.

As we have shown in Sec. IV, for a given concentration of QW excitons $\rho_{2D} \lesssim 10^9$ cm^{-2}, the thermalization kinetics slows down with decreasing T_b/T_0, i.e., with the development of quantum statistics. By increasing both temperatures, T_0 and T_b, and keeping unchanged the ratio $T_0/T_b \gg 1$ one can simultaneously avoid the above bottleneck effect in relaxation and achieve high population of the ground-state mode, $N_{\varepsilon=0} \gg 1$. However, in this case the concentration of excitons, $\rho_{2D} \propto T_0$, increases as well, so that exciton-exciton

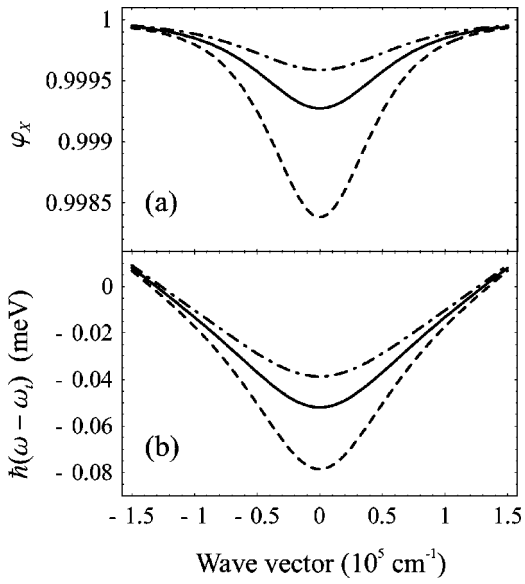

FIG. 8. Possible design of GaAs-based microcavities: (a) excitonic component $\varphi_X=\varphi_X(\mathbf{k}_\parallel)$ of the MC polariton eigenstate and (b) the lower-branch polariton dispersion $\hbar(\omega-\omega_t)$. Detuning $\delta=50$ meV (dashed lines), 75 meV (solid lines), and 100 meV (dash-dotted lines). The energy of ground-state QW excitons is given by $E_{\mathbf{k}_\parallel=0}=\hbar\omega_t=1.522$ eV.

interaction eventually becomes the main mechanism of relaxation in GaAs/Al_xGa_{1-x}As-coupled or ZnSe single QW's.

In contrast, in high-quality GaAs-based microcavities with a relatively large positive detuning $\delta=\hbar(\omega_0-\omega_t)$ between the cavity mode ($\hbar\omega_0$) and QW exciton line ($\hbar\omega_t$) the LA-phonon-assisted kinetics remains dominant even at relatively high degeneracy temperatures $T_0\gg T_b>1$. In these systems, by changing the detuning δ within the band, $\delta=50$–100 meV, one can design an effective in-plane mass M_x so that the bottleneck effect in phonon-assisted scattering, due to the low density of states $\propto M_x$, is already relaxed, whereas the degeneracy temperature $T_0\propto\rho_{2D}/(E_0M_x)$ is still relatively high. Indeed, in such MCs the lower polariton branch gives rise to the in-plane translational mass much smaller than the mass of optically-undressed QW excitons. In the meantime the excitonic component φ_X of the microcavity polaritons is already very high, $\varphi_X\gtrsim0.999$, resulting in the long optical-decay (in the z direction) lifetimes on a time scale of few nanoseconds. This is illustrated in Fig. 8(a), where the detuning δ is equal to 50, 75, and 100 meV. The corresponding polariton (exciton) masses are given by $M_x=0.023\ m_0$, $0.050\ m_0$, and $0.081\ m_0$, respectively. The relevant lower-branch polariton dispersions are plotted in Fig. 8(b). Because the energy E_0 is only on a 0.01 meV energy scale, the parabolic approximation of the lower-branch dispersion curves is valid for low-temperature relaxation kinetics. Thus the LA-phonon-assisted thermalization of the excitonlike MC polaritons can indeed be modeled by the kinetic equations (2.1) and (2.2). Time evolutions of the exciton distribution $N_\varepsilon(t)$, which are typical for the proposed design of GaAs-based MC's, are shown in Fig. 6 (see the plots with $T_b=1$ and 10). Figure 7(a) illustrates the corresponding population dynamics of the ground-state mode, $N_{\varepsilon=0}=N_{\varepsilon=0}(t)$.

For the above-considered GaAs microcavities with detuning $\delta\gtrsim50$ meV, the LA-phonon-assisted relaxation of MC-polaritons is more efficient than the MC-polariton–MC-polariton scattering if

$$\lambda_0=\lambda_0(T_b,T_0)\geqslant\frac{1}{\tau_{\text{p-p}}}=\frac{\pi}{4\hbar}\left(\frac{M_x}{\mu_x}\right)^2E_0T_0, \qquad (5.3)$$

where $\tau_{\text{p-p}}$ is the characteristic time of polariton-polariton scattering and μ_x is the in-plane reduced mass of excitons in a MC-embedded QW (for the details of the above estimate of $\tau_{\text{p-p}}$ see the Appendix of Ref. 10). The rhs of inequality (5.3) shows that $1/\tau_{\text{p-p}}$ is proportional to ρ_{2D}, as it should be due to particle-particle scattering, and to M_x, due to the quasi 2D density of energy states. Note that $\tau_{\text{p-p}}$ is independent of the exciton Bohr radius a_x (or energy), because the exciton-exciton scattering amplitude U_0 is uniquely defined by $U_0\simeq\pi\hbar^2/\mu_x$. The latter result is a direct consequence of the quasi-two-dimensionality of MC polaritons.[10] In the high-temperature limit, $T_0\geqslant T_b\gg1$, of the statistically degenerate MC polaritons analyzed in the previous paragraph, inequality (5.3) holds for concentrations $\rho_{2D}\leqslant(0.5$–$1.0)\times10^9$ cm^{-2}.

VI. CONCLUSIONS

In this paper we have studied thermalization kinetics of statistically degenerate QW excitons coupled to thermal bulk acoustic phonons. For concentrations of QW excitons $\rho_{2D}\lesssim10^9$ cm^{-2} the particle-particle interaction in GaAs or ZnSe QW's can be neglected in comparison with the QW exciton–bulk-acoustic-phonon scattering, and the thermalization kinetics from an initial distribution of QW excitons at $t=0$ occurs through the nonequilibrium states. The following conclusions summarize our results.

(i) For the case of well-developed Bose-Einstein statistics, when $T_b<T_0$ so that $N_{\varepsilon=0}>1$, the relaxation kinetics of QW excitons coupled to thermal bulk acoustic phonons is given by the following scheme. Within a few characteristic scattering times the correlation of the distribution function $N_\varepsilon(t)$ with the initial $N_\varepsilon(t=0)$ disappears, and the subsequent thermalization of QW excitons is described in terms of the adiabatic stage of relaxation. The adiabatic stage is characterized by the start time t_c, which absorbs a gross information about the initial distribution $N_\varepsilon(t=0)$, and by the parameter λ_0, which depends only upon the bath and degeneracy temperatures, T_b and T_0. At the beginning of the adiabatic stage, i.e., for the time domain $0\leqslant t-t_c\lesssim\lambda_0^{-1}$, one has $|N_{\varepsilon\leqslant1/4}-N^0_{\varepsilon\leqslant1/4}|\simeq N^0_{\varepsilon\leqslant1/4}$, and the thermalization kinetics is strongly nonexponential, with $\delta T\propto1/t$ and $N_{\varepsilon=0}\propto(1+\chi t)^\nu$. At large times, when the deviation of the system from the final equilibrium state is already small $[|N_\varepsilon(t)-N^0_\varepsilon|/N^0_\varepsilon\ll1]$, the adiabatic stage of the phonon-assisted thermalization becomes exponential, $\delta T\propto e^{-\lambda_0 t}$, and can be described within the linearized kinetic equation.

(ii) The linearized LA-phonon-assisted kinetics of QW excitons is formulated in terms of the Fredholm integral

equation (4.1). The eigenvalues $\{\lambda\}$ of the collision integral are given by the continuous spectrum $\lambda_0 \leqslant \lambda < \infty$ and the isolated eigenvalue $\lambda = 0$. The marginal eigenvalue $\lambda_0 = \lambda_0(T_b, T_0)$ determines the thermalization time at $t \to \infty$ by $\tau_{\rm th} = \lambda_0^{-1}$. In dependence on the two control parameters, T_b and $T_0 \propto \rho_{\rm 2D}$, the thermalization time achieves two limits: $\tau_{\rm th} \ll \tau_{\rm sc}$ and $\tau_{\rm th} \gg \tau_{\rm sc}$. The eigenfunctions $\psi_\varepsilon(\lambda)$ of the collision integral (4.1) are smooth integrable functions with three isolated critical points in energy space. The critical points of $\psi_\varepsilon(\lambda)$ give rise to a first-order pole, a logarithmic singularity, and a continuous steplike jump.

(iii) Because the LA-phonon-assisted kinetics becomes dominant only at small concentrations of QW excitons, $\rho_{\rm 2D} \lesssim 10^9$ cm^{-2}, nonclassical statistics of quasi-2D excitons in ZnSe or GaAs QW's develops at very low bath temperatures $T_b < 1$ K. The proposed design of GaAs-based microcavities with a relatively large positive detuning between the cavity mode and QW exciton line, $\hbar(\omega_0 - \omega_t) \geqslant 50$ meV, allows us, however, to build up $N_{\varepsilon \simeq 0} \gg 1$ by means of QW exciton–bulk-LA-phonon scattering in much more favorable conditions, i.e., $T_b \gtrsim 1$ K and $\tau_{\rm th} \ll \tau_{\rm sc}$.

ACKNOWLEDGMENTS

We appreciate valuable discussions with L. V. Butov, V. Fal'ko, and M. S. Skolnick. Support of this work by the EPSRC (UK) is gratefully acknowledged.

APPENDIX: TEMPERATURE LAW

In this Appendix we give the expressions for the parameters and functions used in Eqs. (3.11), (3.15), and (3.16). The parameters α_0 and β arise from those terms in the collision integral that contain $f_{\varepsilon \geqslant 1/4}(t)$ and $f^2_{\varepsilon \geqslant 1/4}(t)$, respectively. Collecting such terms together one gets

$$\alpha_0 = \frac{4}{\tau_{\rm sc}\varepsilon_c}\Bigg[\varepsilon_c \int_{\varepsilon_c - 1/4}^{\varepsilon_c} F_{\rm S}(\varepsilon_c, \varepsilon)(1 + n_\varepsilon^{\rm ph} + N^0_{\varepsilon_c - \varepsilon})\varepsilon\, d\varepsilon + \int_0^{\varepsilon_c - 1/4} F_{\rm S}(\varepsilon_c, \varepsilon)(1 + n_\varepsilon^{\rm ph} + N^0_{\varepsilon_c - \varepsilon})\varepsilon^2 d\varepsilon - \int_0^{\infty} F_{\rm AS}(\varepsilon_c, \varepsilon)(n_\varepsilon^{\rm ph} - N^0_{\varepsilon_c + \varepsilon})\varepsilon^2 d\varepsilon\Bigg] \tag{A1}$$

and

$$\beta = \frac{4}{\tau_{\rm sc} T_b}\Bigg[\int_0^{\varepsilon_c - 1/4} F_{\rm S}(\varepsilon_c, \varepsilon)(N^0_{\varepsilon_c - \varepsilon})'(\varepsilon_c - \varepsilon)\varepsilon\, d\varepsilon - \int_0^{\infty} F_{\rm AS}(\varepsilon_c, \varepsilon)(N^0_{\varepsilon_c + \varepsilon})'(\varepsilon_c + \varepsilon)\varepsilon\, d\varepsilon\Bigg]. \tag{A2}$$

The function $\alpha_1(t)$ stems from the terms proportional to $f_{\varepsilon \geqslant 1/4}(t) f_{\varepsilon < 1/4}(t)$ and is given by

$$\alpha_1(t) = \frac{4T_b}{\tau_{\rm sc}} \int_0^{1/4} F_{\rm S}(\varepsilon_c, \varepsilon_c - \varepsilon)(N^0_\varepsilon)' f_\varepsilon(t)(\varepsilon_c - \varepsilon) d\varepsilon. \tag{A3}$$

The parameter $\tilde{\alpha}$ from Eq. (3.13) is obtained by collecting all the terms proportional to $\delta T(t)$,

$$\tilde{\alpha} = -\int_{\varepsilon_c - 1/4}^{\varepsilon_c} F_{\rm S}(\varepsilon_c, \varepsilon)(1 + n_\varepsilon^{\rm ph} + N^0_{\varepsilon_c - \varepsilon}) \frac{\eta(\varepsilon_c - \varepsilon)}{\xi_0(\varepsilon_c - \varepsilon)} \varepsilon\, d\varepsilon - (\alpha_0 \tau_{\rm sc} \varepsilon_c)/(4T_b^2). \tag{A4}$$

When deriving Eq. (3.16) from Eq. (3.15) we first put $\varepsilon = 0$ everywhere in the integrand (3.15) except the exponent. By changing the integration variable ε to $\xi = \xi_0(\varepsilon)$ and putting $\varepsilon = 0$ we derive the asymptotic Eq. (3.16), valid in the limit $t \to \infty$. In this equation $\tilde{\gamma}_0$ is a time-independent prefactor given by

$$\tilde{\gamma}_0 = F_{\rm S}(\varepsilon_c, \varepsilon_c)(1 + n^{\rm ph}_{\varepsilon_c} + N^0_{\varepsilon = 0}) \frac{\varepsilon_c f_{\varepsilon = 0}(t_0)}{\xi_0'(0)}. \tag{A5}$$

*Email address: Alexander.Soroko@astro.cf.ac.uk

[1] For a review of the experimental works on relaxation and photoluminescence kinetics of QW excitons see, e.g., J. Shah, *Ultrafast Spectroscopy of Semiconductors and Semiconductor Nanostructures*, Springer Series in Solid-State Sciences Vol. 115 (Springer, Berlin, 1996).

[2] T. Takagahara, Phys. Rev. B **31**, 6552 (1985).

[3] A. Vinattieri, J. Shah, T.C. Damen, D.S. Kim, L.N. Pfeiffer, M.Z. Maialle, and L.J. Sham, Phys. Rev. B **50**, 10 868 (1994).

[4] P.E. Selbmann, M. Gulia, F. Rossi, E. Molinari, and P. Lugli, Phys. Rev. B **54**, 4660 (1996).

[5] C. Piermarocchi, F. Tassone, V. Savona, A. Quattropani, and P. Schwendimann, Phys. Rev. B **53**, 15 834 (1996).

[6] M. Gulia, F. Rossi, E. Molinari, P.E. Selbmann, and P. Lugli, Phys. Rev. B **55**, R16 049 (1997).

[7] M. Gurioli, P. Borri, M. Colocci, M. Gulia, F. Rossi, E. Molinari, P.E. Selbmann, and P. Lugli, Phys. Rev. B **58**, R13 403 (1998).

[8] F. Tassone and Y. Yamamoto, Phys. Rev. B **59**, 10 830 (1999).

[9] I.K. Oh, J. Singh, A. Thilagam, and A.S. Vengurlekar, Phys. Rev. B **62**, 2045 (2000).

[10] A.L. Ivanov, P.B. Littlewood, and H. Haug, Phys. Rev. B **59**, 5032 (1999).

[11] T.C. Damen, J. Shah, D.Y. Oberli, D.S. Chemla, J.E. Cunningham, and J.M. Kuo, Phys. Rev. B **42**, 7434 (1990).

[12] R. Eccleston, R. Strobel, W.W. Rühle, J. Kuhl, B.F. Feuerbacher, and K. Ploog, Phys. Rev. B **44**, 1395 (1991); R. Eccleston, B.F.

Feuerbacher, J. Kuhl, W.W. Rühle, and K. Ploog, *ibid.* **45**, 11 403 (1992).
[13] T. Fukuzawa, E.E. Mendez, and J.M. Hong, Phys. Rev. Lett. **25**, 3066 (1990). However, the experimental results of this work were later reinterpreted.
[14] L.V. Butov, A. Zrenner, G. Abstreiter, G. Böhm, and G. Weimann, Phys. Rev. Lett. **73**, 304 (1994).
[15] L.V. Butov and A.I. Filin, Phys. Rev. B **58**, 1980 (1998).
[16] L.V. Butov, A. Imamoglu, S.V. Mintsev, K.L. Campman, and A.C. Gossard, Phys. Rev. B **59**, 1625 (1999).
[17] V. Negoita, D.W. Snoke, and K. Eberl, Phys. Rev. B **60**, 2661 (1999).
[18] L.V. Butov, A.L. Ivanov, A. Imamoglu, P.B. Littlewood, A.A. Shashkin, V.T. Dolgopolov, K.L. Campman, and A.C. Gossard, Phys. Rev. Lett. **86**, 5608 (2001).
[19] A.V. Larionov and V.B. Timofeev, Pis'ma Zh. Éksp. Teor. Fiz. **73**, 342 (2001) [JETP Lett. **73**, 301 (2001)].
[20] V.V. Krivolapchuk, E.S. Moskalenko, and A.L. Zhmodikov, Phys. Rev. B **64**, 045313 (2001).
[21] S. Charbonneau, M.L.W. Thewalt, E.S. Koteles, and B. Elman, Phys. Rev. B **38**, 6287 (1988).
[22] A. Alexandrou, J.A. Kash, E.E. Mendez, M. Zachau, J.M. Hong, T. Fukuzawa, and Y. Hase, Phys. Rev. B **42**, 9225 (1990).
[23] J.E. Golub, K. Kash, J.P. Harbison, and L.T. Florez, Phys. Rev. B **41**, 8564 (1990).
[24] J.E. Golub, K. Kash, J.P. Harbison, and L.T. Florez, Phys. Rev. B **45**, 9477 (1992).
[25] F. Clérot, B. Deveaud, A. Chromette, A. Regreny, and B. Sermage, Phys. Rev. B **41**, 5756 (1990).
[26] An average inhomogeneous broadening of indirect excitons in modern high-quality GaAs/Al_xGa_{1-x}As-coupled QW's is less than 0.7 meV and can be further considerably decreased by replacing Al_xGa_{1-x}As alloy in the substrate, barrier QW, and cap layer by pure AlAs [D.W. Snoke (private communication)]. The above value of the inhomogeneous broadening is about one order of magnitude smaller than that observed in the first optical experiments with coupled QW's and is already close to the homogeneous width of about 0.1 meV. The latter is determined by the spectral band of the optically active indirect excitons from the radiative zone $|\mathbf{k}_\parallel| \leqslant (\sqrt{\varepsilon_b} E_{\mathrm{ind}})/(\hbar c)$, where ε_b is the background dielectric constant and E_{ind} is the energy of indirect QW excitons. The existence of large-size, mesoscopic in-plane areas, which are practically free from the disorder effects,[18] is, however, most important for our model of the phonon-assisted relaxation kinetics in high-quality GaAs/Al_xGa_{1-x}As-coupled QW's.
[27] A. Parlangeli, P.C.M. Christianen, J.C. Maan, I.V. Tokatly, C.B. Soerensen, and P.E. Lindelof, Phys. Rev. B **62**, 15 323 (2000).
[28] M. Umlauff, J. Hoffmann, H. Kalt, W. Langbein, J.M. Hvam, M. Scholl, J. Söllner, M. Heuken, B. Jobst, and D. Hommel, Phys. Rev. B **57**, 1390 (1998); H. Kalt, J. Hoffmann, M. Umlauff, W. Langbein, and J.M. Hvam, Phys. Status Solidi B **206**, 103 (1998).
[29] G. Bacher, R. Spiegel, T. Kümmell, R. Weigand, A. Forchel, B. Jobst, D. Hommel, and G. Landwehr, J. Cryst. Growth **184/185**, 330 (1998).
[30] E.A. Uehling and G.E. Uhlenbeck, Phys. Rev. **108**, 1175 (1932).
[31] U. Bockelmann, Phys. Rev. B **50**, 17 271 (1994).
[32] Yu.E. Lozovik and V.I. Yudson, Pis'ma Zh. Éksp. Teor. Fiz. **22**, 556 (1975) [JETP Lett. **22**, 274 (1975)].
[33] X. Zhu, P.B. Littlewood, M. Hybertsen, and T. Rice, Phys. Rev. Lett. **74**, 1633 (1995).
[34] P.B. Littlewood and X. Zhu, Phys. Scr. **68**, 56 (1996).
[35] Y. Naveh and B. Laikhtman, Phys. Rev. Lett. **77**, 900 (1996).
[36] C. Ciuti, P. Schwendimann, B. Deveaud, and A. Quattropani, Phys. Rev. B **62**, R4825 (2000).
[37] P.G. Savvidis, J.J. Baumberg, R.M. Stevenson, M.S. Skolnick, D.M. Whittaker, and J.S. Roberts, Phys. Rev. Lett. **84**, 1547 (2000).
[38] A.I. Tartakovskii, M. Emam-Ismail, R.M. Stevenson, M.S. Skolnick, V.N. Astratov, D.M. Whittaker, J.J. Baumberg, and J.S. Roberts, Phys. Rev. B **62**, R2283 (2000).
[39] F. Boeuf, R. André, R. Romestain, Le Si Dang, E. Péronne, J.F. Lampin, D. Hulin, and A. Alexandrou, Phys. Rev. B **62**, R2279 (2000).
[40] R.M. Stevenson, V.N. Astratov, M.S. Skolnick, D.M. Whittaker, M. Emam-Ismail, A.I. Tartakovskii, P.G. Savvidis, J.J. Baumberg, and J.S. Roberts, Phys. Rev. Lett. **85**, 3680 (2000).
[41] J.J. Baumberg, P.G. Savvidis, R.M. Stevenson, A.I. Tartakovskii, M.S. Skolnick, D.M. Whittaker, and J.S. Roberts, Phys. Rev. B **62**, R16 247 (2000).
[42] P.G. Savvidis, C. Ciuti, J.J. Baumberg, D.M. Whittaker, M.S. Skolnick, and J.S. Roberts, Phys. Rev. B **64**, 075311 (2001).
[43] S.D. Baranovskii, R. Eichmann, and P. Thomas, Phys. Rev. B **58**, 13 081 (1998).
[44] C. Bradford, C.B. O'Donnell, B. Urbaszek, C. Morhain, A. Balocchi, K.A. Prior, and B.C. Cavenett, Phys. Rev. B **64**, 195309 (2001).
[45] A.L. Ivanov, C. Ell, and H. Haug, Phys. Rev. E **55**, 6363 (1997); Phys. Status Solidi B **206**, 235 (1998).
[46] C. Cercignani, *The Boltzmann Equation and Its Applications*, Springer Series in Applied Mathematical Sciences Vol. 67 (Springer, New York, 1988), Sec. IV 6, p. 180.